

UCRL-JC-133759

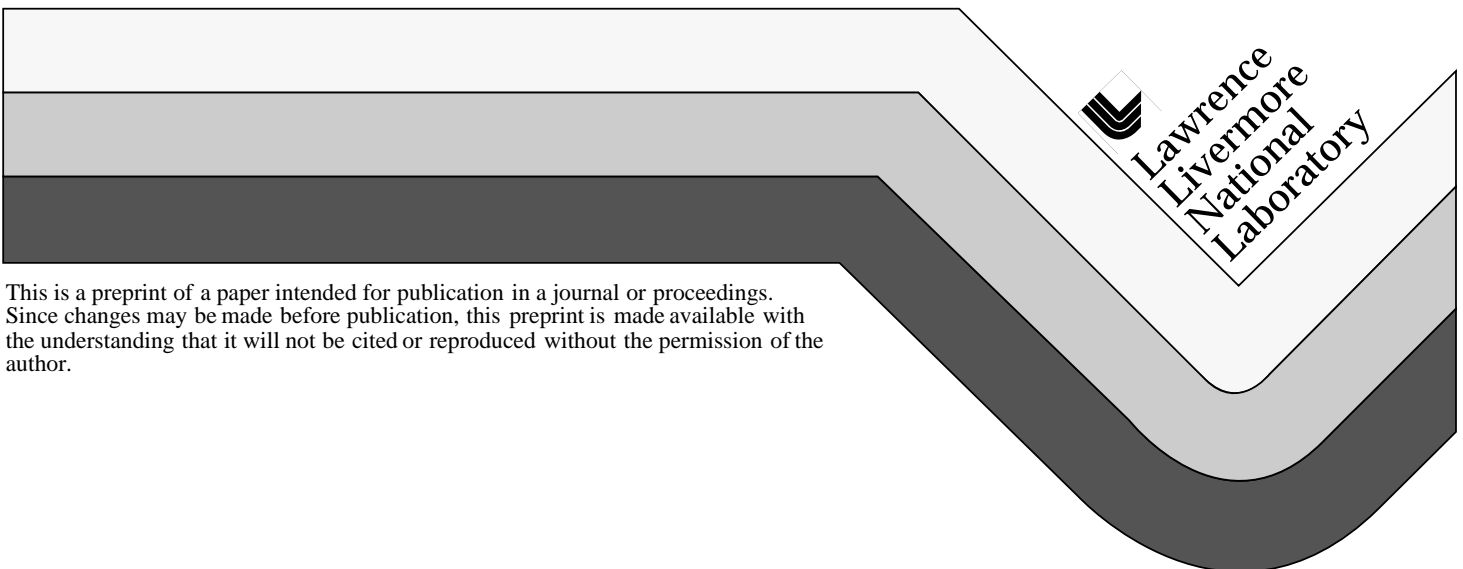
PREPRINT

# **Interface Controlled Deformation Twinning in an Intermetallic Nanolaminate**

L.M. Hsiung  
T.G. Nieh

This paper was prepared for submittal to the  
Sixth International Conference on Composites Engineering  
Orlando, FL  
June 27-July 3, 1999

**March 1999**



#### DISCLAIMER

This document was prepared as an account of work sponsored by an agency of the United States Government. Neither the United States Government nor the University of California nor any of their employees, makes any warranty, express or implied, or assumes any legal liability or responsibility for the accuracy, completeness, or usefulness of any information, apparatus, product, or process disclosed, or represents that its use would not infringe privately owned rights. Reference herein to any specific commercial product, process, or service by trade name, trademark, manufacturer, or otherwise, does not necessarily constitute or imply its endorsement, recommendation, or favoring by the United States Government or the University of California. The views and opinions of authors expressed herein do not necessarily state or reflect those of the United States Government or the University of California, and shall not be used for advertising or product endorsement purposes.

# INTERFACE CONTROLLED DEFORMATION TWINNING IN AN INTERMETALLIC NANOLAMINATE

**L. M. Hsiung and T. G. Nieh**

Lawrence Livermore National Laboratory, L-369, P.O. Box 808, Livermore, CA 94551-9900

## Microstructure

Figure 1 is a bright-field TEM image showing a typical edge-on microstructure within a TiAl ( $\gamma$ )-Ti<sub>3</sub>Al ( $\alpha_2$ ) intermetallic nanolaminate. In general, the material contains two types of interfaces [1]: (1) The  $\gamma/\alpha_2$  interphase interface which has a usual orientation relationship  $(0001)_{\alpha_2} \parallel (111)_{\gamma}$  and  $\langle 11\bar{2}0 \rangle_{\alpha_2} \parallel \langle 1\bar{1}0 \rangle_{\gamma}$ ; (2) The  $\gamma/\gamma$  twin-related interface which includes true-twin ( $180^\circ$  rotational) and pseudo-twin ( $60$  and/or  $120^\circ$  rotational) interfaces. Here, the width of  $\alpha_2$  layers ranges from 10 to 50 nm, and that of  $\gamma$  layers ranges from 150 to 300 nm. Figure 2 is a weak-beam dark-field (WBDF) TEM image showing a typical dislocation substructure within the nanolaminate. Both lattice dislocations (*LD* hereafter) within  $\gamma$  layer and a high density of interfacial dislocations (*ID* hereafter) on inclined interfaces can be clearly seen. The density of *ID* is much greater than that of *LD*, and the *LD* are primarily threading dislocations which terminate their two ends at the interfaces. While the *ID* on semi-coherent  $\gamma/\alpha_2$  and  $\gamma/\gamma$  pseudo-twin interfaces are  $1/6\langle 112 \rangle$  or  $1/3\langle 112 \rangle$  type misfit dislocations [2], the on  $\gamma/\gamma$  true-twin interface are mainly  $1/6[11\bar{2}]$  type twinning dislocations or geometry necessary dislocations for accommodating the departure of true-twin interface from the exact (111) twin plane.

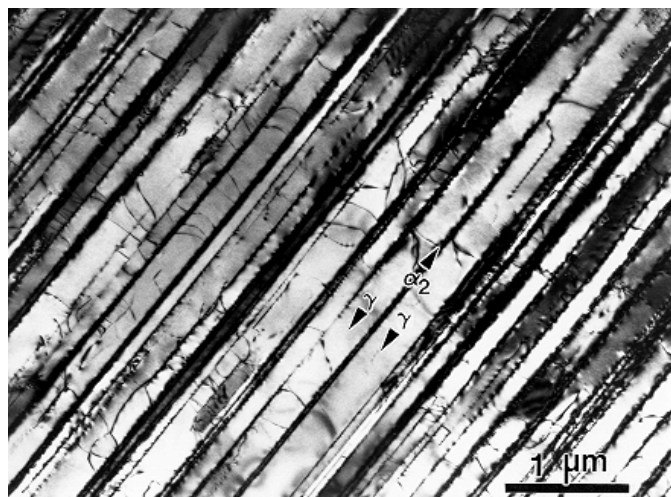


Fig. 1. Bright-field TEM image showing a lamellar grain viewing from an edge-on orientation.

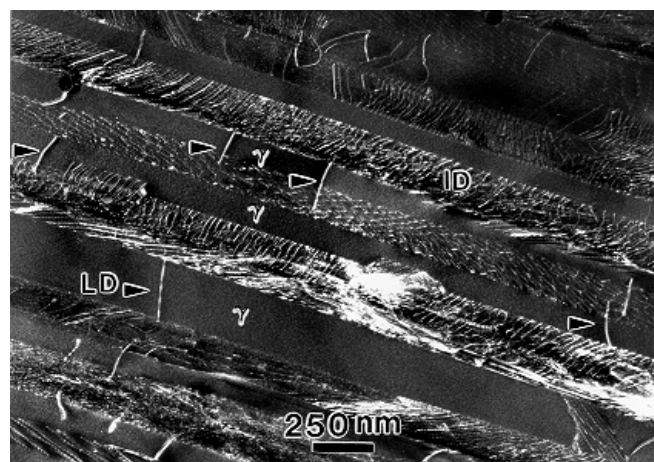


Fig. 2. WBDF image showing a typical dislocation structure of an inclined nanolaminate.

## Deformation twinning and proposed mechanisms

When the nanolaminate was creep deformed at  $760^\circ\text{C}$  and 518 MPa, a deformation substructure associated with deformation twins (*DT* hereafter) within  $\gamma$  layers was developed. A typical example of the formation of  $(\bar{1}11)[211]$ -type *DT* within the nanolaminate is shown in Fig. 3 (a). It is noted that one of the twin lamellae was still growing between two lamellar interfaces, and its growth would be eventually terminated by the lower interface. This observation suggests that the interfaces are preferred nucleation sites for *DT*, presumably resulting from the high local stresses caused by the pileup of *ID*. Accordingly, it is proposed that deformation twinning in the TiAl-Ti<sub>3</sub>Al nanolaminate can be viewed as a stress relaxation process to relieve the local stress concentration caused by the pile-up of interfacial dislocations during deformation. The effective stress ( $\tau_e$ ) at the tip of the pile-up of  $n$  dislocations can be evaluated by  $\tau_e = n\tau_i$  [3], where  $\tau_i$  is the resolved shear stress acting on the interface. To relieve the stress

concentration, deformation twinning in  $\gamma$  layers is therefore taking place by a dislocation reaction based upon a stair-rod cross-slip mechanism [4,5]. As for an example of the  $(\bar{1}11)$ -type DT formed in the nanolaminate, the corresponding dislocation reaction (dissociation) is proposed to be  $1/6[\bar{1}2\bar{1}]_{(111)} \rightarrow 1/6[011]_{(100)} + 1/6[\bar{1}\bar{1}2]_{(\bar{1}11)}$ . The  $(\bar{1}11)$ -type DT is accordingly formed by a successive cross-slip of the twinning dislocations  $1/6[\bar{1}\bar{1}2]$  on the  $(\bar{1}11)$  plane and leaving the stair-rod dislocations  $1/6[011]$  on the (100) plane. Twin (stacking) faults are subsequently formed on the interfaces between the  $\gamma$  layer and DT. This is schematically illustrated in Fig. 3 (b).

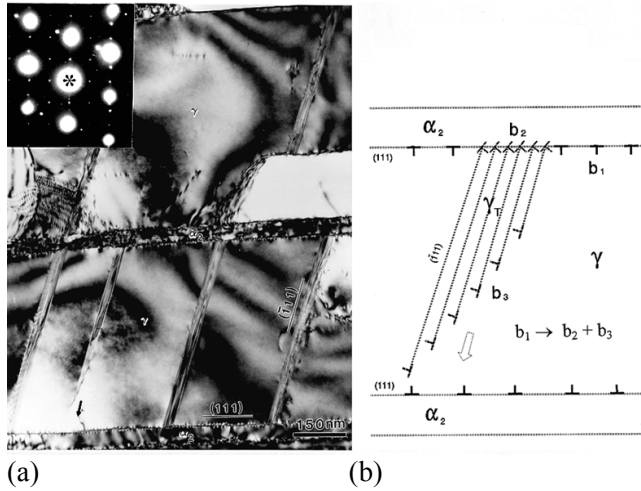


Fig. 3. (a) A bright-field TEM image showing several  $(\bar{1}11)$  type deformation twins formed during growth process toward another interface. (b) Schematic illustration of the nucleation of a  $(\bar{1}11)$  type DT from a  $\gamma/\alpha_2$  interface, where  $b_1$ ,  $b_2$ , and  $b_3$  denote the interfacial, stair-rod, and twinning dislocations, respectively.

The formation of stair-rod dislocations at the intersections between the DT and  $\alpha_2$  layer is evidenced in Fig. 4, where the array of  $1/6[011]$  stair-rod dislocations become invisible [Fig. 4(a)] or visible [Fig. 4(b)] when a reflection vector ( $g$ )  $200$  or  $021$  is used for imaging. It is noted that the individual stair-rod dislocation is not resolvable because of a narrow distance (0.25 nm) between two stair-rod dislocations. The significance of the proposed mechanism is to reveal that there are several barriers to be overcome in order to activate the twinning reaction. These barriers include (1) the repulsive force ( $F$ ) between the interfacial (Shockley) and stair-rod dislocations, (2) the increase of line energy due to the dislocation dissociation, and (3) the increase of interfacial energy due to the formation of twin faults. Among them the

repulsive force ( $F$ ) between the interfacial (Shockley) and stair-rod dislocations is considered to be rate controlling. That is, a critical (minimum) stress ( $\tau_c$ ) is required to activate the dissociation reaction for twinning.

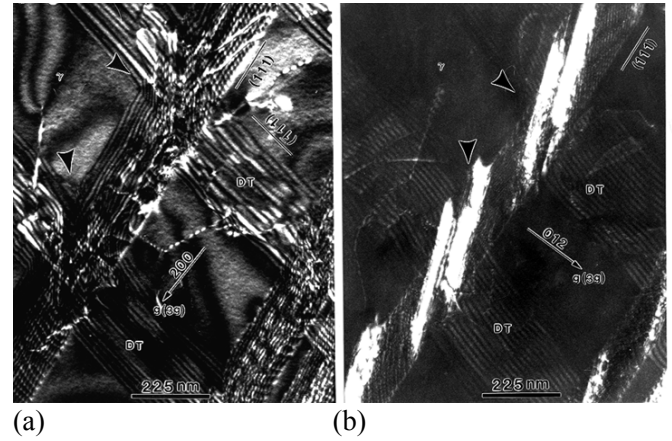


Fig. 4. Paired WBDF images demonstrating the existence of the array of  $1/6[011]$  stair-rod dislocations at the intersections (indicated by arrows) between the  $(\bar{1}11)$ -type DT and  $\alpha_2$  layer. (a) Invisible at  $g = 200$  ( $g \cdot b = 0$ ), (b) visible at  $g = 021$ ,  $Z$  (zone axis)  $\approx [0\bar{1}2]$ .

### Acknowledgments

This work was performed under the auspices of the U.S. Department of Energy through contract # W-7405-Eng-48 with Lawrence Livermore National Laboratory. The authors would like to thank Dr. C. T. Liu of Oak Ridge National Laboratory for providing P/M materials for this study.

### References

1. M. Yamaguchi and Y. Umakoshi, *Progress in Materials Science*, **34**, p. 1 (1990).
2. L.M. Hsiung and T.G. Nieh, *Mater. Sci., & Engrg.*, **A239-240**, p. 438 (1997).
3. J.D. Eshelby, F.C. Frank and F.R.N. Nabarro, *Phil. Mag.*, **42**, p. 351 (1951).
4. Fujita and T. Mori, *Scripta Metall.*, **9**, p. 631 (1975).
5. T. Mori and H. Fujita, *Acta Metall.*, **28**, p. 771 (1980).